The refractive index of silver nanowire networks : a heuristic approach to the foundations of the optical constants, from experiment to theory.

Supporting Information

Amaury Baret[1], Julia Baumgarten[1,2], François Balty[1,2], Frédéric Rabecki[3], Jérémy Brisbois[3], Buyun Zheng[4], Daniel Bellet[4] and Ngoc Duy Nguyen[1]

1) Experimental methods

Silver nanowires in IPA solutions were purchased from ACS materials, with average solution diameters of 40, 60, 90 and 120 nm. Based on experimental results from Balty *et al.*[1], the announced values by the supplier fall within expected standard deviation, validating the reliability of the vendor's diameter specifications for these samples and justifying the use of the nominal diameters as input parameters to the models. The solutions were spray-coated onto cleaned Corning glass substrates which was simultaneously heated to 110 °C to facilitate IPA evaporation. In-situ resistance measurements were employed to indirectly control the deposition density. Optical transmittance and reflectance spectra were measured using a Lambda 1050 UV/Vis/NIR spectrophotometer with an integrating sphere. The feature observed in the optical spectra at $\lambda = 2200$ nm corresponds to an experimental artifact associated with a defect in the spectralon of the spectrophotometer. The areal mass density *amd* of the samples was determined via SEM imaging. From the SEM images, the density was extracted using the ImageJ plugin Ridge Detection[2]. The results were associated with a 20% measurement error, accounted for throughout the study. To deduce the *amd* from the areal filling fraction f_A obtained via the Ridge Detection algorithm, we used the following formula that stems directly from its definition:

$$amd = \rho_{Ag} \times c \times f_A \times D_{NW},$$

where $\rho_{Ag} = 10490\ \mathrm{kg/m^3}$ is the mass density of bulk silver, D_{NW} is the average nanowire diameter, and with

$$c = \frac{5}{16 \sin^2(54°) \tan(36°)}$$

a dimensionless geometrical factor relating the areal section of a pentagonal (the shape of AgNW fabricated using the widespread polyol process) nanowire to its diameter[3].

[1] SPIN, Department of Physics, , University of Liège, Liège, Belgium. E-mail : abaret@uliege.be
[2] EPNM, Department of Physics, University of Liège, Liège, Belgium
[3] CSL, Centre Spatial de Liège, Liège, Belgium
[4] Univ. Grenoble Alpes, CNRS, Grenoble INP, LMGP, F-38000 Grenoble, France

2) Effective refractive indices of AgNW networks on glass

Previous studies on the refractive indices (RIs) of silver nanowire (AgNW) networks have utilized *Eqs.* (1) and (2) from the main manuscript to determine the effective RIs of AgNW networks on glass substrates. For reference, these equations are restated here :

$$k = \frac{\lambda}{4\pi d}\ln\left(\frac{1-R}{T}\right) \qquad (1)$$

$$n = \frac{1+R}{1-R} + \sqrt{\frac{4R}{(1-R)^2} - k^2} \qquad (2)$$

As discussed, *Eq.* (S2) is applicable to dielectric materials, a category under which the hybrid (AgNW/glass) structure can reasonably be assumed to fall. We note that *Eq.* (S2) assumes negligible reflectance at the rear interface and is valid for semi-transparent films where interference effects are not considered. Applying these equations to our measured spectra yields the real refractive index values shown in Fig. S1. We note that the thickness of the AgNW layer was taken as twice the diameter of the NWs given that real networks are never truly 2D and have a higher thickness due to NWs overlapping. While the exact value of 2 for this factor is an approximation, it is of the right order of magnitude given the densities considered in this work and is kept constant through the whole research.

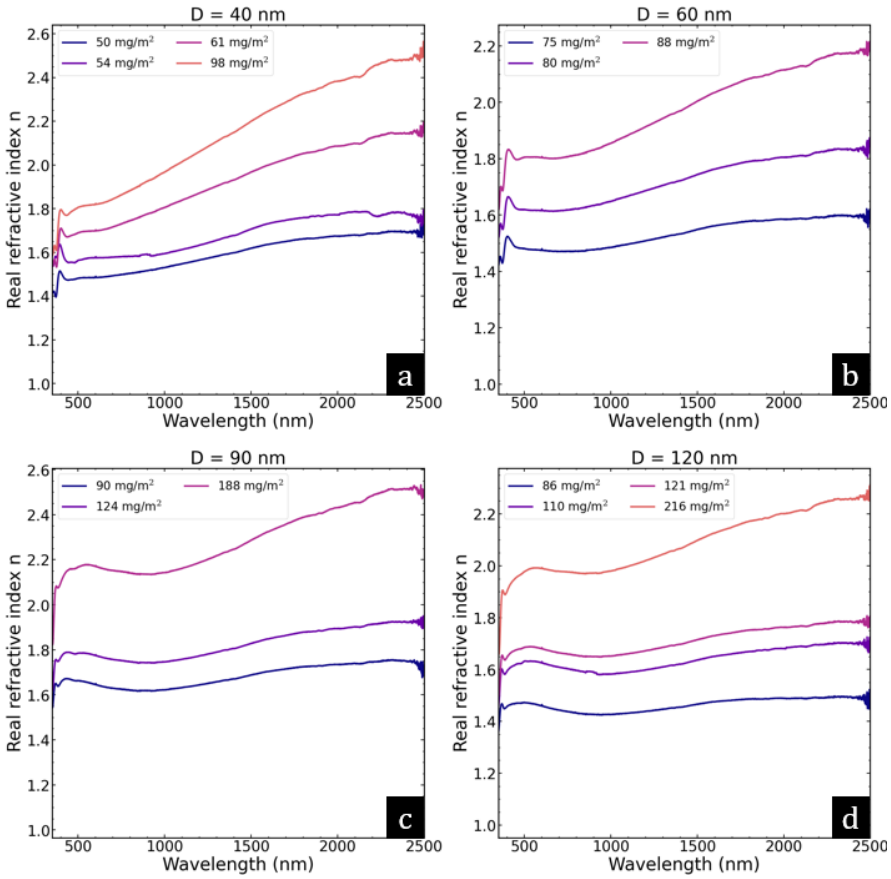

Fig. S1. Real refractive index as a function of the wavelength of the hybrid (AgNW/glass) structure, as calculated via Eq. S2 and for samples of varying *amd* and average nanowire diameters of *(a)* 40 nm, *(b)* 60 nm, *(c)* 90 nm, *(d)* 120 nm.

All spectra remain strictly above $n = 1$, confirming the expected dielectric behavior. The trends in n reflect those of the measured reflectance spectra, consistent with the form of *Eq.* S2. Larger-

diameter nanowires exhibit flatter spectral behavior with wavelength, while smaller diameters show greater variation. Additionally, denser networks correspond to higher refractive indices, aligning with the intuitive prediction that denser structures deviate further from air's refractive index. These results agree well with prior studies, both in trends and absolute values[4–7], supporting the reliability of our measurements.

Using the RIs derived from Fig. S1 and the Fresnel and Beer-Lambert equations described in the main manuscript, we calculated the predicted transmittance of the AgNW/glass samples. These predictions were compared to the experimental transmittance obtained via spectrophotometry. Since *Eqs.* S1 and S2 are derived from Fresnel's equations, this process effectively validates the internal consistency of the approach. The close agreement between predicted and measured transmittance confirms the suitability of this method for describing the effective optical properties of AgNW networks on glass substrates (but glass substrates alone). Consequently, it is important to note that the transmittance analyzed here corresponds to the AgNW/glass samples, not the isolated networks themselves.

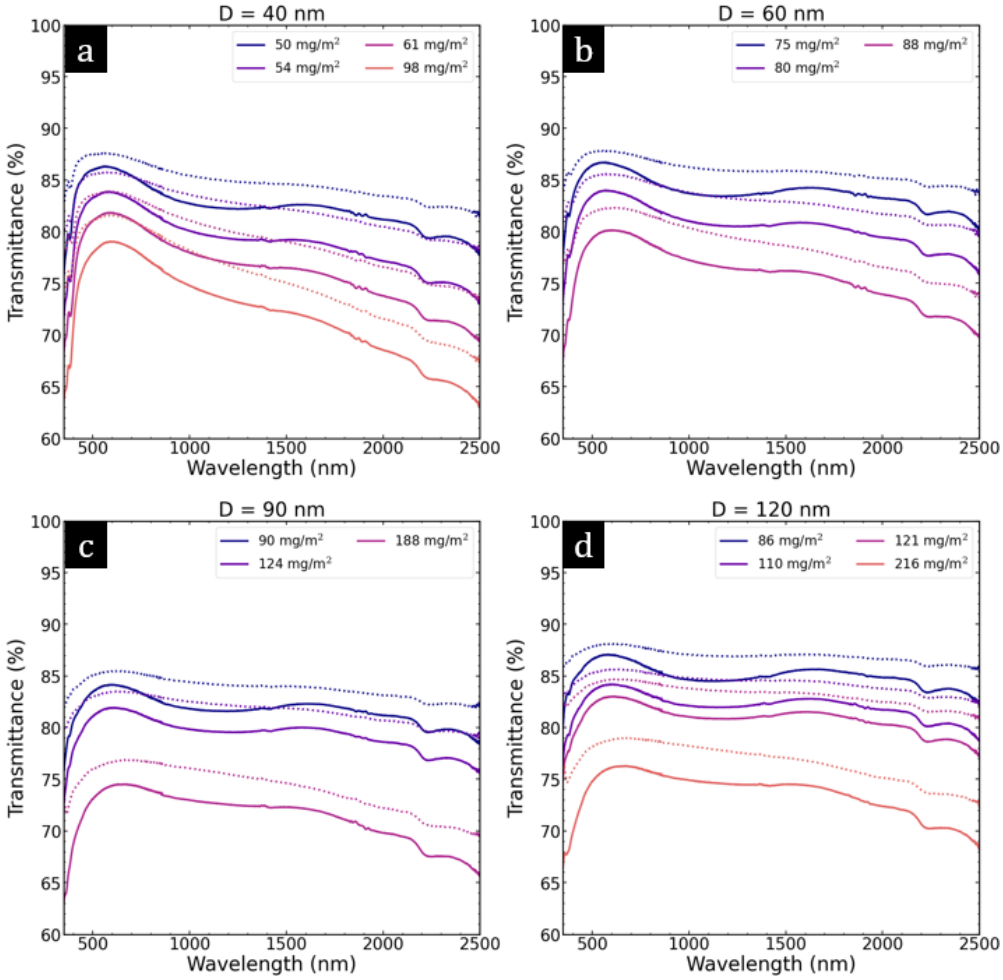

Fig. S2. Optical transmittance spectra as a function of the wavelength of the hybrid (AgNW/glass) structure, for samples of varying *amd* and average nanowire diameters of *(a)* 40 nm, *(b)* 60 nm, *(c)* 90 nm, *(d)* 120 nm. Solid lines correspond to the experimentally measured transmittance, whereas dashed lines correspond to the calculated transmittance from the effective RIs.

While we consider these results insightful as they allow one to easily predict the transmittance of AgNW networks on glass, we believe they suffer from two major limitations:

• n, k curves are solely derived from the measured R,T curves and cannot be used to predict the refractive indices of a sample without corresponding measurements.

• These results describe the AgNW/glass hybrid system, not the network alone. As a result, they cannot be used to extract the intrinsic optical properties of the nanowire networks or to predict

their optical behavior on substrates other than glass. Yet, a wide range of mechanically flexible materials, such as PET, can serve as substrates to AgNW networks for innovative flexible applications.

3) Details on Mie's and van de Hulst' theories implementation

For an infinite cylinder of radius r_{cyl} made of a material of refractive index $\tilde{n} = n + ik$, the associated Mie coefficients are given by[8]:

$$a_n = \frac{J_n(\alpha)J_n'(\tilde{n}\alpha) - \tilde{n}J_n(\tilde{n}\alpha)J_n'(\alpha)}{H_n^{(2)}(\alpha)J_n'(\tilde{n}\alpha) - \tilde{n}J_n(\tilde{n}\alpha)H_n^{(2)\prime}(\alpha)}$$
$$b_n = \frac{\tilde{n}J_n(\alpha)J_n'(\tilde{n}\alpha) - J_n(\tilde{n}\alpha)J_n'(\alpha)}{\tilde{n}H_n^{(2)}(\alpha)J_n'(\tilde{n}\alpha) - J_n(\tilde{n}\alpha)H_n^{(2)\prime}(\alpha)}$$

, where $\alpha = \frac{2\pi}{\lambda} \times r_{cyl}$ is the size parameter, J_n is the Bessel function of the first kind of nth order, J_n' is the 1st derivative of the former with respect to α, and $H_n^{(2)}$ is the Hankel function of the second kind of order n, with $H_n^{(2)\prime}$ its 1st derivative with respect to α. In our work, these functions were computed using the *scipy.special* functions *jv*, *jvp, hankel2,* and *h2vp*, respectively[9].
Given these coefficients, the scattering coefficients at normal incidence for *s* and *p*-polarized light can be computed as[10]:

$$S_s(0) = a_0 + 2\sum_{n=1}^{n_{max}} a_n$$

$$S_p(0) = b_0 + 2\sum_{n=1}^{n_{max}} b_n$$

, with $n_{max} = \mathrm{int}(\alpha + 4.05\,\alpha^{1/3} + 2)$.d
From the knowledge of these scattering coefficients, vdH's model predicts the composite RIs of a material of refractive index $\tilde{n}_{matrix}$ in which are embedded the nanostructures with a volumetric fraction f_v:

$$n_{\mathrm{hybrid}}(\lambda) = n_{\mathrm{matrix}}(\lambda)\left(1 + \frac{f_v\lambda^2}{2\pi^2 cD^2}\,\mathrm{Im}[S(0)]\right)$$
$$k_{\mathrm{hybrid}}(\lambda) = k_{\mathrm{matrix}}(\lambda)\,\frac{f_v\lambda^2}{2\pi^2 cD^2}\,\mathrm{Re}[S(0)]$$

, where $S(0) = 0.5 \times \left(S_s(0) + S_p(0)\right)$, D is the cylinder's diameter, and c the geometrical constant introduced in section *S*1. In this work, we set $\tilde{n}_{\mathrm{matrix}} = \tilde{n}_{\mathrm{air}} = 1$ and the hybrid is thus the AgNW network itself.

4) Robustness of the model to input parameters

a. On the presence of PVP around the Ag NWs

It is well known that due to the polyol process of fabrication of the Ag NWs, polyvinylpyrrolidone (PVP), used as a capping agent during their synthesis, is present as a thin layer surrounding the wires and could, in principle, affect the optical response of the network. According to the supplier (ACS Materials), the PVP content is below 0.5 wt%. While this low concentration suggests a limited contribution, it is not sufficient by itself to justify neglecting its effect. More importantly, as the PVP layer has a significant optical response above λ=2000 nm, we would expect this to manifest as distinct features in the measured transmittance and reflectance spectra. However, no such spectral signatures are observed in our measurements. We interpret this result as an indication that the influence of PVP on the overall optical response of the networks can be neglected. On the basis of this interpretation, we consider it reasonable to exclude PVP from the model without compromising its accuracy.

b. Equivalent network thickness

We have performed a study that assesses how the assumed equivalent thickness of the nanowire network - defined as the number of superimposed nanowires seen in cross-section - affects the modeled optical response. The value of $2D_{NW}$ used throughout the manuscript was chosen as a conservative lower-bound estimate, based on visual inspection of SEM images, such as the one shown in Fig. S3 below.

To evaluate the sensitivity of the model with respect to this parameter, we ran simulations for several values of the equivalent thickness, ranging from 2 to 4 nanowire diameters. The resulting transmittance and reflectance spectra are shown in Fig. S4. While the exact equivalent thickness has not been measured, this parametric study shows that the model remains robust to variations in this assumption. Using a value of $2D_{NW}$ provides a lower-bound estimate, and increasing this number slightly improves the agreement with experimental results without altering the fundamental conclusions of the study. This result reinforces the applicability of the Mie + van de Hulst model for predicting the optical properties of silver nanowire networks.

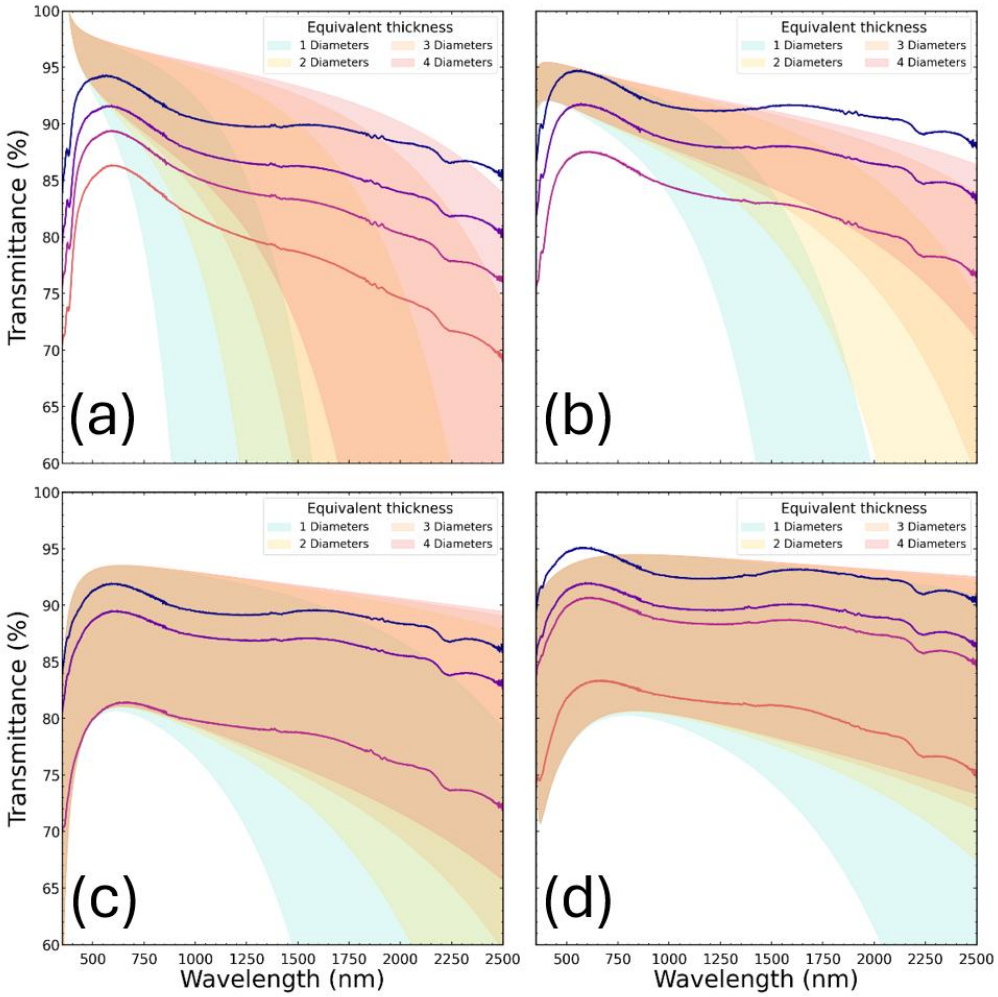

Optical transmittance as a function of the wavelength for AgNW networks with average nanowire diameters of *(a)* 40 nm, *(b)* 60 nm, *(c)* 90 nm, and *(d)* 120 nm. Thin lines show experimentally measured transmittances at various densities, while shaded areas represent simulation results using the Mie+vdH model for a range of equivalent network thicknesses. The density ranges used in the simulations match those in the original manuscript, corresponding to the minimum and maximum measured densities with a $\pm$ 20% margin.

While a deeper exploration of the relationship between network density and effective thickness could further refine the model, such an investigation is beyond the scope of the present study.

c. Areal mass density exactness

The amd is a critical parameter for characterizing AgNW networks. However, its precise determination is challenging due to the nature of the samples: the networks are deposited on electrically insulating glass substrates, which hinders the clarity of SEM images. As a result, direct measurement of amd is not straightforward. The 20% uncertainty reported in the main text stems from an empirical evaluation of the SEM images. Specifically, the threshold parameters for automatic nanowire identification were varied to match visually determined "minimum" and "maximum" nanowire counts, which correlated well with manual identification. Obtaining an exact value of the amd would require a significant amount of work and remains difficult in practice. Therefore, for this study, an estimated value combined with a conservative error margin was considered sufficient

Given the inherent uncertainty in amd determination, the impact of density variability on the model predictions was also assessed. Model calculations were performed assuming perfect knowledge of the density (*i.e.*, without applying any error margin). While this idealized scenario is unlikely to be perfectly exact, it provides insight into the robustness of the modeling approach. Even under this extreme assumption, the model remains consistent for networks composed of larger-diameter nanowires, supporting the original conclusion that the model is valid when nanowire diameters are sufficiently large compared to the wavelength of light.

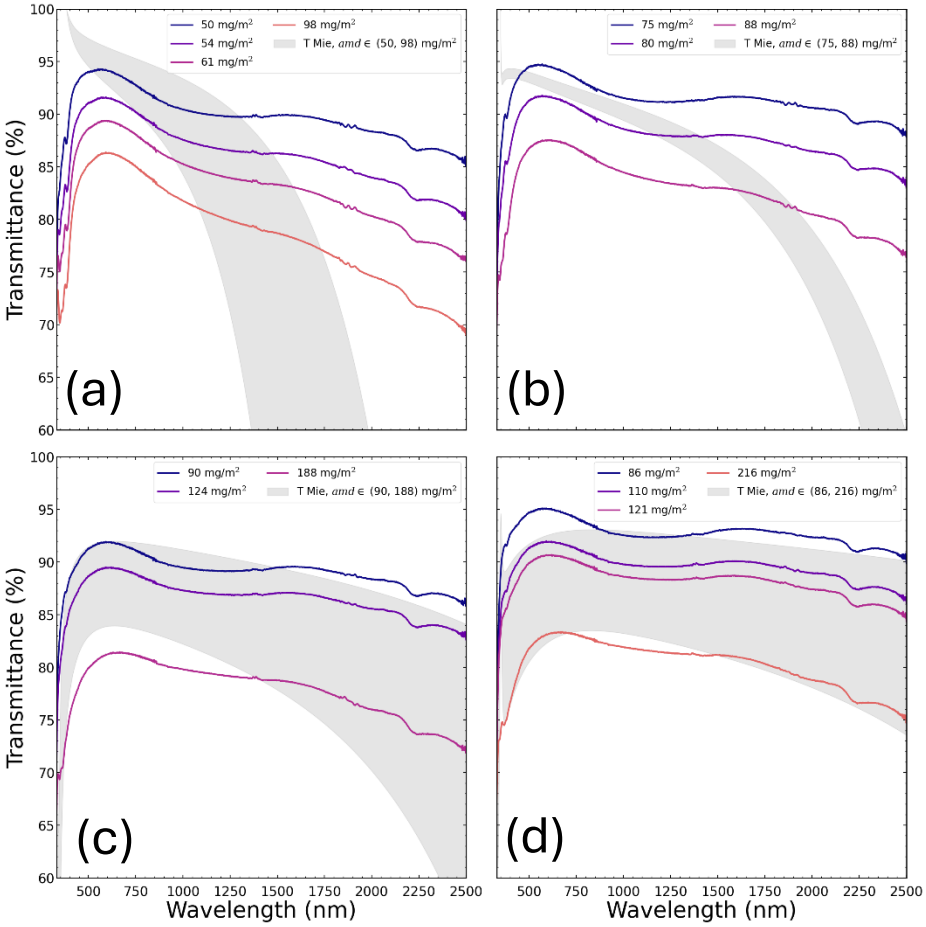

Optical transmittance as a function of the wavelength for AgNW networks with average nanowire diameters of *(a)* 40 nm, *(b)* 60 nm, *(c)* 90 nm, and *(d)* 120 nm. Thin lines show experimentally measured transmittances at various densities, while shaded areas represent simulation results using the Mie+vdH model for a range of amds corresponding to the minimum and maximum measured values, without any error margin accounted for.

To estimate the effective optical constants of the silver nanowire network, it is also possible to use different mixing models, such as the well-known Maxwell garnett effective medium theory. We show below the results of such a model applied to infinite cylinders, considered as anisotropic inclusions in a dielectric matrix of air. In this formulation, the silver nanowires are treated as inclusions with complex permittivity ϵ_{Ag} embedded in a dielectric matrix with permittivity ϵ_{Air} . The anisotropic nature of the cylinders is captured by averaging over depolarization factors L for different directions: $L = [0,0.5,0.5]$, corresponding to the longitudinal and transverse directions of the wires[11]. An effective polarizability γ_{pol} is computed by summing the directional contributions:

$$\gamma_{pol} = \frac{1}{3}\sum_{i=1}^{3}\frac{\epsilon_{Ag} - \epsilon_{Air}}{\epsilon_{Air} + L_i(\epsilon_{Ag} - \epsilon_{Air})}$$

This polarizability is then used in the Maxwell-Garnett formula to compute the composite permittivity:

$$\epsilon_{net} = \epsilon_{Air}\frac{1 + \frac{2}{3}f_v\gamma_{pol}}{1 - \frac{1}{3}f_v\gamma_{pol}}$$

where f_v is the volume filling factor of the nanowires in the matrix. Finally, the complex refractive index is retrieved as:

$$n_{net} + ik_{net} = \sqrt{\epsilon_{net}}$$

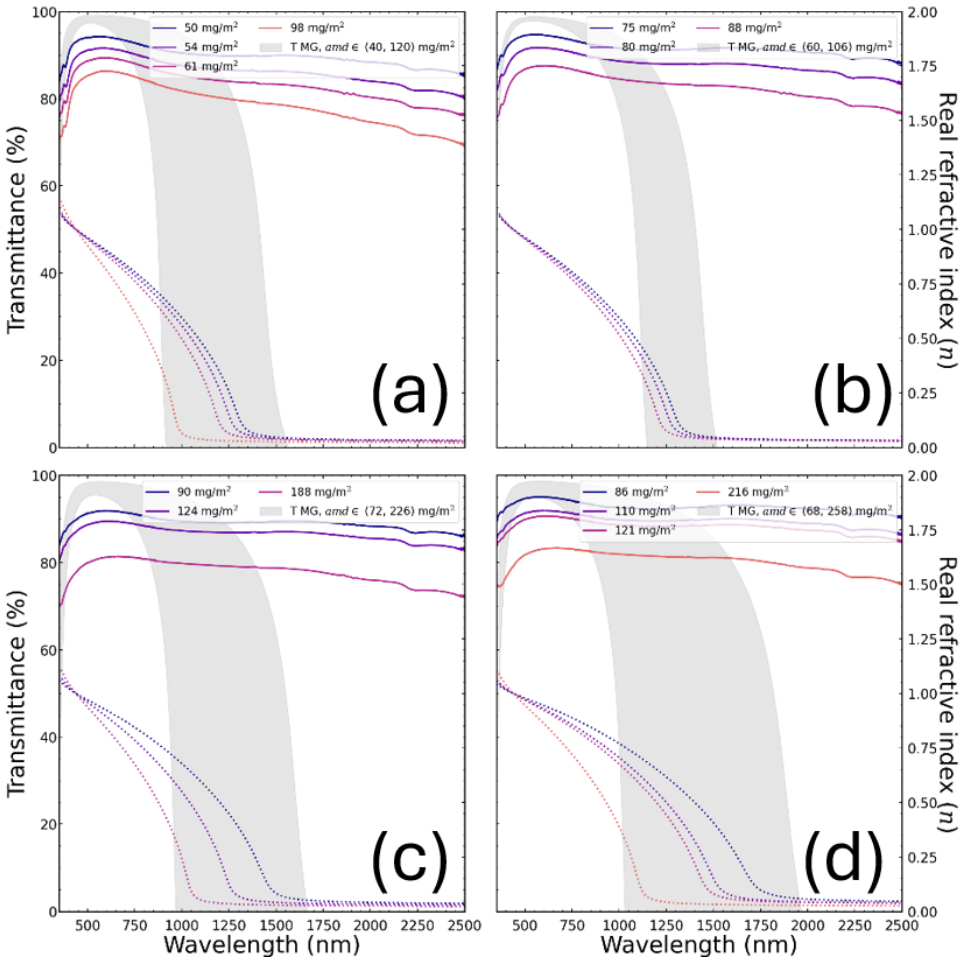

Optical transmittance as a function of the wavelength for AgNW networks with average nanowire diameters of *(a)* 40 nm, *(b)* 60 nm, *(c)* 90 nm, and *(d)* 120 nm. Thin lines show experimentally measured transmittances at various densities, while shaded areas represent simulation results using the Maxwell Garnett (MG) model for a range of $amds$ corresponding to the minimum and maximum measured values $\pm 20\%$. The dashed lines correspond to the real part of the refractive index, n.

As can be observed, while the MG model yields transmittance values that are in rough agreement with experimental data in the visible range, it quickly breaks down in the near-infrared region. Specifically, the model fails beyond ~1200 nm due to the refractive index n approaching zero, a nonphysical result. Even within the visible spectrum, the MG model provides less accurate predictions than the vdH model, which is consistent with the observations reported in the paper by Khanarian *et al*.

These results further validate our choice of the vdH model as a more robust and accurate framework for describing the optical response of AgNW networks, especially when extending the analysis into the near-infrared.

References

(1) Balty, F.; Baret, A.; Silhanek, A.; Nguyen, N. D. Insight into the Morphological Instability of Metallic Nanowires under Thermal Stress. *Journal of Colloid and Interface Science* **2024**, *673*, 574–582. https://doi.org/10.1016/j.jcis.2024.06.074.

(2) Wagner, T.; Hiner, M.; xraynaud. Thorstenwagner/Ij-Ridgedetection: Ridge Detection 1.4.0, 2017. https://doi.org/10.5281/zenodo.845874.

(3) Lagrange, M. Physical Analysis of Percolating Silver Nanowire Networks Used as Transparent Electrodes for Flexible Applications. phdthesis, Université Grenoble Alpes, 2015. https://tel.archives-ouvertes.fr/tel-01266300 (accessed 2021-10-11).
(4) Yu, X.; Yu, X.; Zhang, J.; Chen, L.; Long, Y.; Zhang, D. Optical Constants of Long Silver Nanowire Thin Films on Glass Calculated from the Transmission Spectra. *Materials Letters* **2017**, *194*, 152–155. https://doi.org/10.1016/j.matlet.2017.02.044.
(5) Tomiyama, T.; Yamazaki, H. Optical Anisotropy Studies of Silver Nanowire/Polymer Composite Films with Mueller Matrix Ellipsometry. *Applied Surface Science* **2017**, *421*, 831–836. https://doi.org/10.1016/j.apsusc.2017.01.152.
(6) Khanarian, G.; Joo, J.; Liu, X.-Q.; Eastman, P.; Werner, D.; O'Connell, K.; Trefonas, P. The Optical and Electrical Properties of Silver Nanowire Mesh Films. *Journal of Applied Physics* **2013**, *114* (2), 024302. https://doi.org/10.1063/1.4812390.
(7) Abdel-Rahim, R. D.; Nagiub, A. M.; Pharghaly, O. A.; Taher, M. A.; Yousef, E. S.; shaaban, E. R. Optical Properties for Flexible and Transparent Silver Nanowires Electrodes with Different Diameters. *Optical Materials* **2021**, *117*, 111123. https://doi.org/10.1016/j.optmat.2021.111123.
(8) Kerker, M. CHAPTER 6 - Scattering by Infinite Cylinders. In *The Scattering of Light and Other Electromagnetic Radiation*; Kerker, M., Ed.; Physical Chemistry: A Series of Monographs; Academic Press, 1969; Vol. 16, pp 255–310. https://doi.org/10.1016/B978-0-12-404550-7.50012-9.
(9) Virtanen, P.; Gommers, R.; Oliphant, T. E.; Haberland, M.; Reddy, T.; Cournapeau, D.; Burovski, E.; Peterson, P.; Weckesser, W.; Bright, J.; van der Walt, S. J.; Brett, M.; Wilson, J.; Millman, K. J.; Mayorov, N.; Nelson, A. R. J.; Jones, E.; Kern, R.; Larson, E.; Carey, C. J.; Polat, İ.; Feng, Y.; Moore, E. W.; VanderPlas, J.; Laxalde, D.; Perktold, J.; Cimrman, R.; Henriksen, I.; Quintero, E. A.; Harris, C. R.; Archibald, A. M.; Ribeiro, A. H.; Pedregosa, F.; van Mulbregt, P. SciPy 1.0: Fundamental Algorithms for Scientific Computing in Python. *Nat Methods* **2020**, *17* (3), 261–272. https://doi.org/10.1038/s41592-019-0686-2.
(10) Appendix C: Normally Illuminated Infinite Cylinder. In *Absorption and Scattering of Light by Small Particles*; John Wiley & Sons, Ltd, 1998; pp 491–497. https://doi.org/10.1002/9783527618156.app4.
(11) Li, S.-Y.; Niklasson, G. A.; Granqvist, C. G. Nanothermochromics: Calculations for VO2 Nanoparticles in Dielectric Hosts Show Much Improved Luminous Transmittance and Solar Energy Transmittance Modulation. *Journal of Applied Physics* **2010**, *108* (6), 063525. https://doi.org/10.1063/1.3487980.